Agronomy Research **16**(X), xxx–ccc, 2018
https://doi.org/10.15159/AR.18.010

Strawberry leaf surface temperature dynamics measured by thermal camera in night frost conditions

E. Kokin*, M. Pennar, V. Palge and K. Jürjenson

Estonian University of Life Sciences, Institute of Technology, Department of Energy Application, Kreutzwaldi 56, EE51014 Tartu, Estonia
*Correspondence: eugen.kokin@emu.ee

Abstract. The aim of the study was to define the strawberry leaf surface and ambient air temperature differences in night frost conditions. The study was carried out at the commercial strawberry field in late autumn at a specific natural climatic situation, corresponding to night frost conditions. Thermal camera FLIR P660 was used for obtaining thermal images and corresponding visual colour images of the strawberry leaves. The images were taken at ten-minute interval. The ambient air temperature, relative humidity, dew point, solar radiation and wind speed data were obtained by Davis Vantage Pro2 weather station. It was estimated that the surface temperature of the specific leaf is comparatively similar at different parts of the specimen and changes noticeably with the variation of solar radiation intensity. The speed of temperature changes was also analysed. During all the measurement period, the considerable difference between the temperature of the leaf and the ambient air temperature was established, especially in absence of solar radiation. The difference of the leaf surface and ambient air temperature reached 8 °C. The study showed that in night frost conditions the plants might be endangered by low temperatures even at the air temperatures above 0 °C due to intensive energy loss by long wave radiation to the sky. It is suggested that the thermal imaging or infrared radiation measurement should be used simultaneously with air temperature measurements for more exact timing of night frost prevention measures at strawberry cultivation.

Key words: thermal imaging, strawberry leaf, surface temperature, night frost conditions, precision agriculture.

INTRODUCTION

The last three decades of twenties century were productive concerning the research works that aimed to find the suitable model for describing the balancing energy flow in radiative night frost conditions. The discussion was evolving around the plants' heat balance components (Businger, 1965; Hamer, 1986; Perry, 1986 and others). Though the models could differ significantly by their outcomes, the modelling gave in practice good results in plants survival rate at low temperatures and because of that, new, improved theories were not developed. Today it seems that for the most effective and widely used sprinkler-protection frost prevention methods there were mainly analyses of their application rates suggested but the subject of exact timing of these measures was not studied thoroughly. As a result, mostly the air temperatures were monitored and used

as an alert criteria but not the temperatures of plant surfaces, that may differ from the air temperatures (Perry, 1994).

The advancements in development of infrared (IR) measurement instruments and technique made it possible to apply IR thermometers and cameras for thermographic measurements of plants. These were mainly the laboratory instruments, which were used for physiological processes analysis in different plants (Jones et al., 2003; Maes et al., 2012 and Costa et al., 2013). Later, these methods were applied also in open-air conditions. The results of thermal radiation measurements made in natural environment by Aubrecht et al. (2016) showed that at high positive temperatures of air in daytime the surface temperature of plant might be higher than air temperature. Though already Perry (1994) suggested that the surface temperature of plants in radiative night frost conditions might be lower than the air temperature by 1.6 to 2.7 °C, the dynamics of plants' temperature dependences on radiative heat exchange were not analysed.

The main objective of our research is to find more exact surface temperature variations in case of strawberry leaf in field experiment at radiative frost conditions using the measurement possibilities of IR thermography.

Theoretical aspects

All heat energy calculations for night frost conditions, where the intensity of additional heat flux needed for description of heat flows of plant parts is sought, are presented by heat balance equations of different forms (Businger, 1965; Hamer, 1986; Perry, 1986 and others).

In this work here, we described the heat balance of strawberry leaf as

$$m_l \cdot c_l \cdot \frac{dT_l}{d\tau} = E_n - C - H \,, \tag{1}$$

where m_l is leaf mass, kg; c_l – specific heat capacity of leaf material, J kg^{-1} K^{-1}; dT_l – leaf temperature change within the time step, K; $d\tau$ – time step, s; E_n – net radiant flux of leaf surface, W; C – sensible heat flow of the leaf, W and H – latent heat flow of the leaf, W (Jones et al., 2011).

The components of Eq. 1 were defined as

$$\begin{aligned} E_n &= E_{\uparrow l} + E_{\downarrow sky} + E_{\downarrow l} + E_{\uparrow ground} = \\ &= 2 \cdot F_l \cdot \varepsilon_l \cdot \sigma \cdot T_l^4 + F_l \cdot \varepsilon_{sky} \cdot \sigma \cdot T_{sky}^4 + F_l \cdot \varepsilon_{soil} \cdot \sigma \cdot T_{soil}^4 , \end{aligned} \tag{2}$$

$$C = 2 \cdot F_l \cdot k_l \cdot \left(T_l - T_a\right), \tag{3}$$

$$H = \frac{2 \cdot F_l \cdot L \cdot \beta \cdot}{R_w \cdot T_l} \cdot \left(e_l - e_a\right). \tag{4}$$

Here $E_{\uparrow l}$, $E_{\downarrow sky}$, $E_{\downarrow l}$, $E_{\uparrow ground}$ are total radiant fluxes emitted from the leaf to sky, sky to leaf, leaf to ground and ground to leaf; σ – Stefan-Boltzmann constant; ε_l, ε_{sky}, ε_{soil} – emissivity of strawberry leaf, sky and soil; T_l, T_{sky}, T_{soil} – absolute temperatures of leaf, sky and surface of soil; F_l – leaf surface area; k_l – heat transfer coefficient between leaf and surrounding air; T_a – air temperature; L – latent heat of vaporization; R_w – specific gas constant for water vapour; β – coefficient of mass transfer; e_l – vapour pressure at leaf surface; e_α – vapour pressure of the surrounding air. For simplification, the radiation angle factors were not included.

Inserting Eq. 2, Eq. 3 and Eq. 4 into Eq. 1, we got the heat balance equation for the leaf in a form that is more complex:

$$m_l \cdot c_l \cdot \frac{dT_l}{d\tau} = 2 \cdot F_l \cdot \varepsilon_l \cdot \sigma \cdot T_l^4 + F_l \cdot \varepsilon_{sky} \cdot \sigma \cdot T_{sky}^4 + F_l \cdot \varepsilon_{soil} \cdot \sigma \cdot T_{soil}^4 + \\ + 2 \cdot F_l \cdot k_l \cdot (T_l - T_a) + \frac{2 \cdot F_l \cdot L \cdot \beta}{R_w \cdot T_l \cdot} \cdot (e_l - e_a). \quad (5)$$

The purpose of this work was to monitor T_l changes in time. From Eq. 5, it is possible to derive T_l and find the changes of its value analytically. In practice, this method is not very reliable, as the sky and soil temperatures are defined in a different way by different authors and therefore might be the cause for errors. It is more convenient to measure each component of the heat balance separately and to define the leaf temperature from measurement results.

Thermal camera visualizes the temperature of measurement object based on the radiant flux (in comparatively narrow long wave spectrum region that corresponds to infrared radiation) and in that case, we do not need the whole heat balance equation (Eq. 1) but only one of its components $E_{\uparrow l}$ from Eq. 2. to establish the temperature of the leaf (T_l).

Infrared thermography

The IR camera work principle can be described by the heat balance of the camera IR sensor (Usamentiaga et al., 2014), as

$$E_{n\,sensor} = E_l + E_{refl} + E_{atm}, \quad (6)$$

$$E_l = \varepsilon_l \cdot \tau_{atm} \cdot \sigma \cdot T_l^4, \quad (7)$$

where $E_{n\,sensor}$ is the net radiant flux to camera sensor; E_l – radiant flux from the leaf to the sensor depending on the leaf surface temperature; E_{refl} – radiant flux reflected to the sensor from the leaf surface; E_{atm} – radiant flux emitted to the sensor by the atmosphere and τ_{atm} – the atmosphere transmissivity between the leaf and the camera. We can write out these components as

$$E_{refl} = (1 - \varepsilon_l) \cdot \tau_{atm} \cdot \sigma \cdot T_{refl}^4, \quad (8)$$

$$E_{atm} = (1 - \tau_{atm}) \cdot \sigma \cdot T_{atm}^4, \quad (9)$$

where T_{refl} is temperature corresponding to reflected radiant flux and ε_l is leaf surface emissivity.

In our experiments, the distance between camera and leaf is about 0.5 m, so we can choose the transmissivity of the atmosphere τ_{atm}= 1. That means that E_{atm}= 0 and the variables influencing the net radiant flux to camera sensor and thus measured temperature value are only T_l, T_{refl} and ε_l. The leaf surface emissivity is suggested to be ε_l = 0.95 (Aubrecht et al., 2016).

The objectives of our work are:

1. To find weather the thermographic measurements by IR camera are applicable for monitoring the temperature of strawberry leaf surface in radiative night frost conditions.
2. To measure the strawberry leaf surface and surrounding air temperatures, to define and analyse their variation in time and to compare their levels.
3. To find out if the air and dew point temperature measurements are sufficient for leaf temperature estimation, and to assess the significance of camera measurement error in IR thermogram analysis.
4. To assess the suitability of the thermography temperature measurement method to be used for the more exact estimation of night frost alerts moments and prevention measures application timing.

MATERIALS AND METHODS

The current study of strawberry leaves' surface temperature was carried out using thermal camera (FLIR P660) with thermal sensitivity 30 mK and accuracy ± 1 K for obtaining thermal images of leaves and ground surface (soil surface without vegetation on the same image with the leaves) with corresponding visual colour images. The sensing system of the camera is based on 640×480-pixel Focal Plane Array uncooled microbolometer perceiving thermal radiation with wavelength 7.5–13 μm (IR) and allowing to measure temperature at more than 40,000 points on the leaf surface. The camera calibrated temperature range of –40.0 °C up to +120.0 °C was used. The images were taken at ten-minute interval from 0.5 m distance and analysed with FLIR ResearchIR Max software (version 4.30.3.76). The ambient air temperature (°C), relative humidity (%), dew point (°C), solar radiation (W m^{-2}) and wind speed (m s^{-1}) data were obtained by weather station (Davis Vantage Pro2) at 2 m above the ground. During calibration of the camera and preliminary measurements, the mean emissivity of strawberry leaves was found to be 0.96. The temperature units, used in the results presentation, are (°C) for temperature values and (K) for speed of change of temperature.

Temperature correction was applied, using ambient air temperature, relative humidity and reflected temperature based on the measured infrared radiant flux reflected to the camera from the surface of the target (Standard test methods for measuring and compensating for reflected temperature using infrared imaging radiometers, 1998; FLIR, 2011).

For achievement of broached objectives, the measurements were carried out on three successive days in late autumn (19.10.2016 to 21.10.2017) at the commercial field of Fragaria×Ananassa 'Sonata' on the three leaves of the same plant planted in May, 2016. The specific natural climatic situation corresponded to night frost conditions. The days and nights were cloudless, the air temperature at the experimental area was around +7 °C in daytime and down to –5.0 °C at night. The wind speed was 0.0 to 2 m s^{-1}. To minimize the effect of additional radiation sources and to prevent the IR radiation shading, the camera was controlled remotely. Thermal images were taken with the camera fixed on a tripod approximately from distance of 50 cm and at an angle of 30 degrees from the leaf surface normal.

From the point of view of the resulting influence of plant leaf radiative balance on the leaf temperature, based on preliminary measurements, the time of the day during the sunset and immediately after it is most informative. At that time, the solar radiation diminishes quickly and the leaf temperature may become lower than ambient air temperature due to exposure to the cloudless sky with temperatures (T_{sky}) below – 50.0 °C (outside of calibrated temperature range of camera).

Fig. 1 shows the strawberry plant thermal image with three leaves. The thermogram is supplied with the temperature scale in °C and three ellipse-shaped and one polygon ROI with corresponding names. The temperature distribution histogram of the selected ROI is also shown.

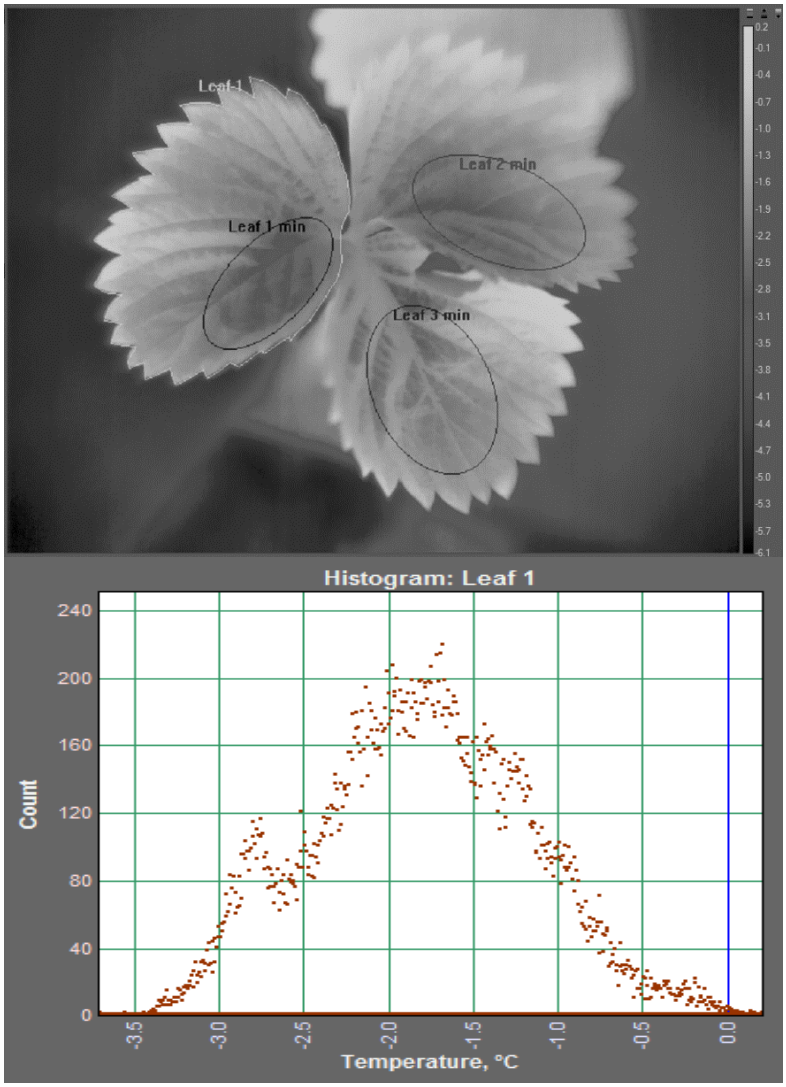

Figure 1. Strawberry leaves' thermal image and selected area (ROI *Leaf 1*) temperature distribution histogram.

Strawberry leaf is complex. It consists of a base, petiole and three leaves. The leaf surface is not uniform – it is divided by veins into angular lamina regions of different size with individual inclination angles to the horizontal plane. The leaf itself is divided into halves by midrib, which is lower than adjoining regions. The result of such surface unevenness is IR radiant flux variation to and from the surface of the leaf and consequently, different leaf surface temperature (T_l) at different parts. For the analysis of T_l the regions of interest (ROI) on the surface of the leaf were selected on thermal images and contoured by the coloured lines, to define the areas with lowest temperatures as most endangered in case of night frost. The number of pixels in these areas were 8,140 to 12,539 – three to four times less than the whole leaf ROI area with 41,150 pixels (Table 1). The ground surface ROI included 1,824 measurement points. The temperature inside the selected ROIs was more uniform and its difference with the whole leaf ROI stayed nearly constant. In all images the area, shape and position of the ROIs were constant (Table 1).

Table 1. Statistical analysis results of thermal image as presented by FLIR ResearchIR Max software for selected areas: *Leaf 1* – the ROI of whole Leaf 1 and *Leaf 1 min*, *Leaf 2 min* and *Leaf 3 min* – ROIs of minimum temperature areas on Leaf 1, 2 and 3 correspondingly

Statistic	ROI *Leaf 1*	ROI *Leaf 1 min*	ROI *Leaf 2 min*	ROI *Leaf 3 min*	ROI *Ground*
Mean, °C	–1.5	–2.4	–2.1	–1.7	–5.9
Std. Dev., °C	0.6	0.2	0.2	0.5	0.2
Centre, °C	–1.3	–2.4	–2.5	–1.7	–5.9
Maximum, °C	0.4	–1.6	–1.3	–0.8	–5.4
Minimum, °C	–3.4	–-3.2	–2.9	–2.7	–6.4
Number of Pix	41,150	8,140	10,733	12,539	1,824
Emissivity	0.96	0.96	0.96	0.96	0.96
Distance, m	0.5	0.5	0.5	0.5	0.5

The FLIR ResearchIR Max software enables to apply the temperature correction procedures and performs the statistical analysis of the thermal images based on selected ROIs data. The resulting information includes the temperature distribution histograms and numerical values for minimum, maximum and mean temperatures and standard deviation for the temperature inside the ROI.

In Table 1 the numerical values of statistical analysis results of thermal image pixel temperatures for four selected areas of the leaves as presented as given by FLIR ResearchIR Max software. Three of these areas with minimal surface temperatures were selected as most endangered. For the final analysis, the ROI with minimum temperatures (*Leaf 1 min*) was used. The correlation analysis was performed using MS Office Excel software.

RESULTS AND DISCUSSION

Perry (1994) suggested that the surface temperature of plants in radiative night frost conditions might be lower than the air temperature by 1.6 to 2.7 °C. Some later research works describe possibilities of determining the leaf emissivity by IR thermometry (Chiachung Chen, 2015), changes of IR spectra of plants caused by stress (Maria F. Buitrago et al., 2016) and early detection of it by IR techniques (Laury Chaerle et al.,

2000). But no results of temperature dynamics in night frost conditions were yet published.

Our measurement series gives the possibility to see the strawberry leaf surface temperature and other measured parameters change starting from 15:10, 19.10.2016 and up to 24:00, 19.10.2016. In Table 2, the numerical results of statistical analysis of thermograms describe the most essential period from 17:00 to 20:20 for ROI *Leaf 1*, with 8,140 pixels. The ground surface mean temperature is also included. This measurement period corresponds to T_{leaf} rapid diminishing to 0 °C at the sunset while the air temperature reaches 0 °C only three hours later.

Table 2. Thermal images statistical analysis results for ROI *Leaf 1* and ground surface temperatures from 17:00 to 20:20, 18.10.2016

Time	Ground surface mean temperature, °C	Leaf surface temperatures, °C				
		minimum	maximum	mean	ROI central point	standard deviation
17:00	–1.3	0.6	2.9	1.5	1.4	0.5
17:10	–2.1	–0.9	1.0	0.0	0.0	0.4
17:20	–3.4	–2.9	–0.9	–2.1	–2.0	0.4
17:30	–5.6	–3.8	–2.0	–3.0	–2.9	0.4
17:40	–6.4	–3.9	–1.9	–3.1	–3.0	0.3
17:50	–6.8	–4.3	–2.7	–3.5	–3.4	0.3
18:00	–7.2	–4.5	–3.2	–3.9	–3.8	0.2
18:10	–8.1	–5.1	–3.6	–4.3	–4.5	0.3
18:20	–7.3	–4.5	–3.3	–3.8	–3.8	0.2
18:30	–8.6	–5.8	–4.5	–5.2	–5.4	0.2
18:40	–8.6	–5.9	–4.7	–5.3	–5.5	0.2
18:50	–9.6	–7.1	–6.0	–6.6	–6.7	0.2
19:00	–9.9	–7.1	–5.7	–6.5	–6.5	0.2
19:10	–10.3	–8.0	–6.9	–7.5	–7.6	0.2
19:20	–10.3	–5.4	–4.4	–4.9	–5.0	0.2
19:30	–10.9	–7.3	–6.3	–6.9	–7.0	0.2
19:40	–11.3	–7.6	–6.8	–7.2	–7.3	0.1
19:50	–11.5	–7.9	–6.9	–7.4	–7.4	0.1
20:00	–11.9	–8.4	–7.3	–7.7	–7.9	0.1
20:10	–12.3	–8.4	–7.6	–7.9	–8.0	0.1
20:20	–12.2	–8.5	–7.6	–8.0	–8.0	0.1

The analysis results of measurement series of leaf's surface temperatures along with the weather station data are presented on Fig. 2. The weather station data is shown for the period of 24 hours while T_l measurements start at 15:10 and end at midnight. The minimum, maximum and mean temperature variations of one ROI is shown along with variations of ground surface and ambient air temperatures, air relative humidity, dew point temperature and solar radiation.

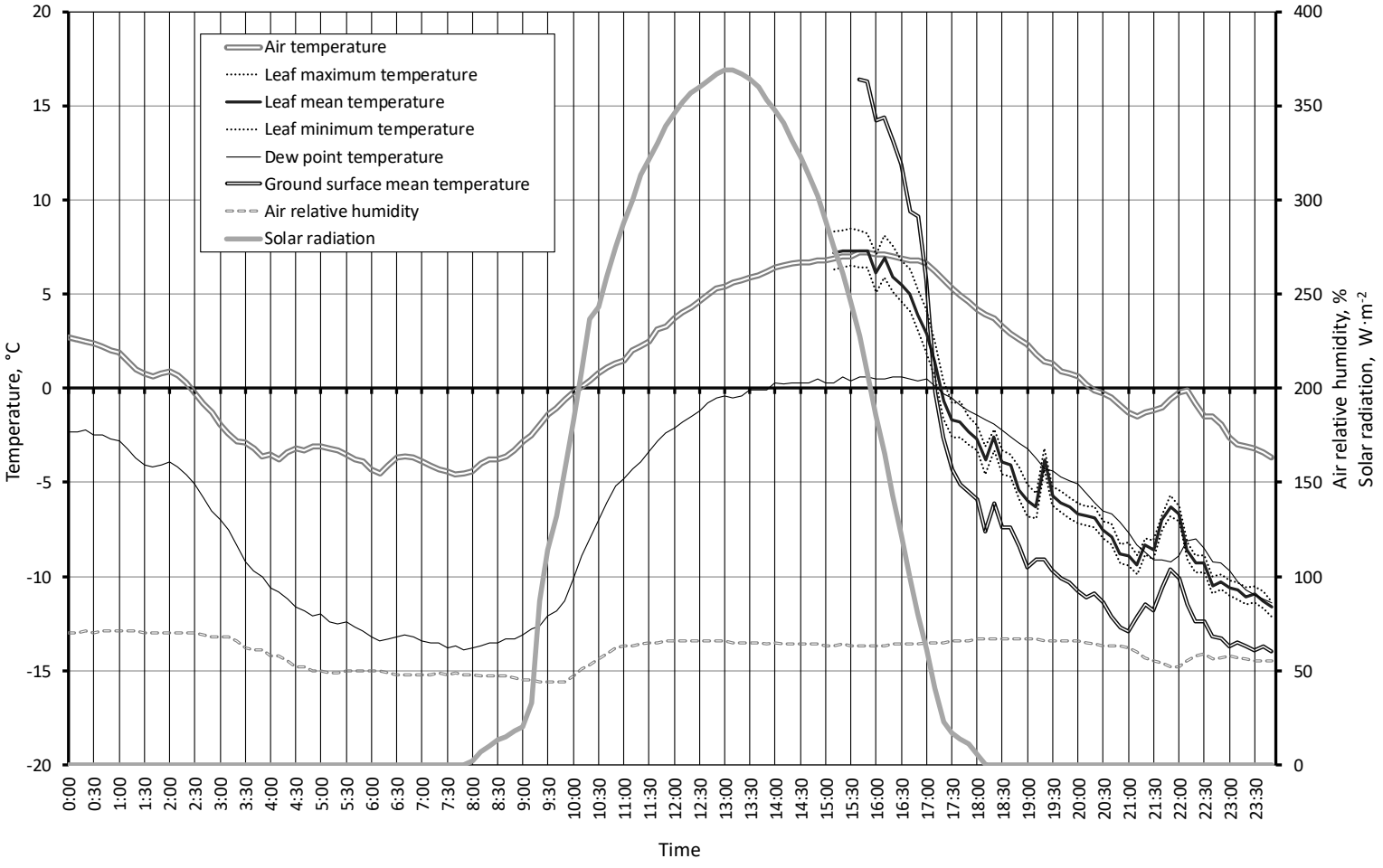

Figure 2. Strawberry leaf's surface temperature variations in night frost conditions.

We can see that the mean value of leaf surface temperature ($T_{l\,mean}$) being close to the air temperature up to 16:20 starts to decrease quickly with the diminishing of solar radiation and reaches 0 °C at 17:10 to 17:20. The air temperature at that moment is still +6.8…+6.0 °C and stays positive up to 20:20. After reaching 0 °C at 17:20, $T_{l\,mean}$ continues to diminish and at 20:20 is already –7.6 to –8.5 °C. We also see that starting from 17:20, $T_{l\,mean}$ is considerably lower than the dew point temperatures. The leaf temperature quick lessening is a result of the radiative heat flow to the cloudless sky, while the radiative heating by the sun is rapidly diminishing. The positive air temperature is not high enough to compensate by convection the radiant heat loss to the sky.

At 16:30 and later, the leaf temperature changes correlates with the solar radiation intensity, and after it diminishes to zero, the $T_{l\,mean}$ correlates to the air temperature, but stays considerably lower both at air positive and negative temperatures. Short-time variations of $T_{l\,mean}$ during measurements may be caused by changes of IR radiant flux to the sky depending on atmosphere transmission. There are also some additional factors, such as the freezing process of dew, condensed on the leaf surface.

Example of that intensive freezing we probably see as horizontal line on the graph at 17:30. We may also suppose, that at some lower temperatures the process of supercooling in plants may cause short-time rise of leaf surface temperature. We see suitable peak at 19:10 when $T_{l\,mean}$ is –7.5 °C. Corresponding temperature peak of ground surface is absent on the graph. That may mean that there are some other causes for rise of leaf surface temperature than IR radiation variation. Though we registered similar peaks on other days also, this hypothesis needs further investigation.

After 17:30, the change of plant temperature is highly correlated to air (r = 0.959) and ground surface (r = 0.988) temperatures. We may notice that on the graph, the changes of $T_{l\,mean}$ and ground surface temperature at 21:50 slightly precede the rise of air temperature. As the air was practically still, we can suggest that the variations of air temperature after sunset were caused mainly by cooling of the surface of the ground because of IR radiation.

The difference of temperatures between leaf and ground surfaces are explainable by the convective heat-exchange between the leaf and surrounding air. The stem of the plant is about 10 cm high and air can freely move around the leaf and thanks to its small mass warm it to some extent.

The temperature differences between the air and strawberry leaf and between the air and ground surface and their variations are shown on Fig. 3. The difference increase nearly linearly until 17:30 and then becomes more stable, changing only with fluctuation of IR radiant flux, with slight rising trend. One of the possible causes for that may be the forming of ice crystals on the surfaces that prevent further temperature difference rapid increase.

In Fig. 4, the speed of leaf temperature changes during the test is shown. The highest speeds coincide with the temperature peaks and reach 0.25 °C min^{-1} (15 °C h^{-1}).

The test results show, that the surface temperature of strawberry leaf in night frost conditions is much lower than air temperature and this difference reaches 8 to 9 °C at air positive temperatures. It means, that the plant temperature is below 0 °C already immediately before the sunset and after it. While it is not so dangerous for the strawberry leaves that can withstand lower temperatures without serious damage it may be fatal for the flowers of the plant if such conditions occur in springtime.

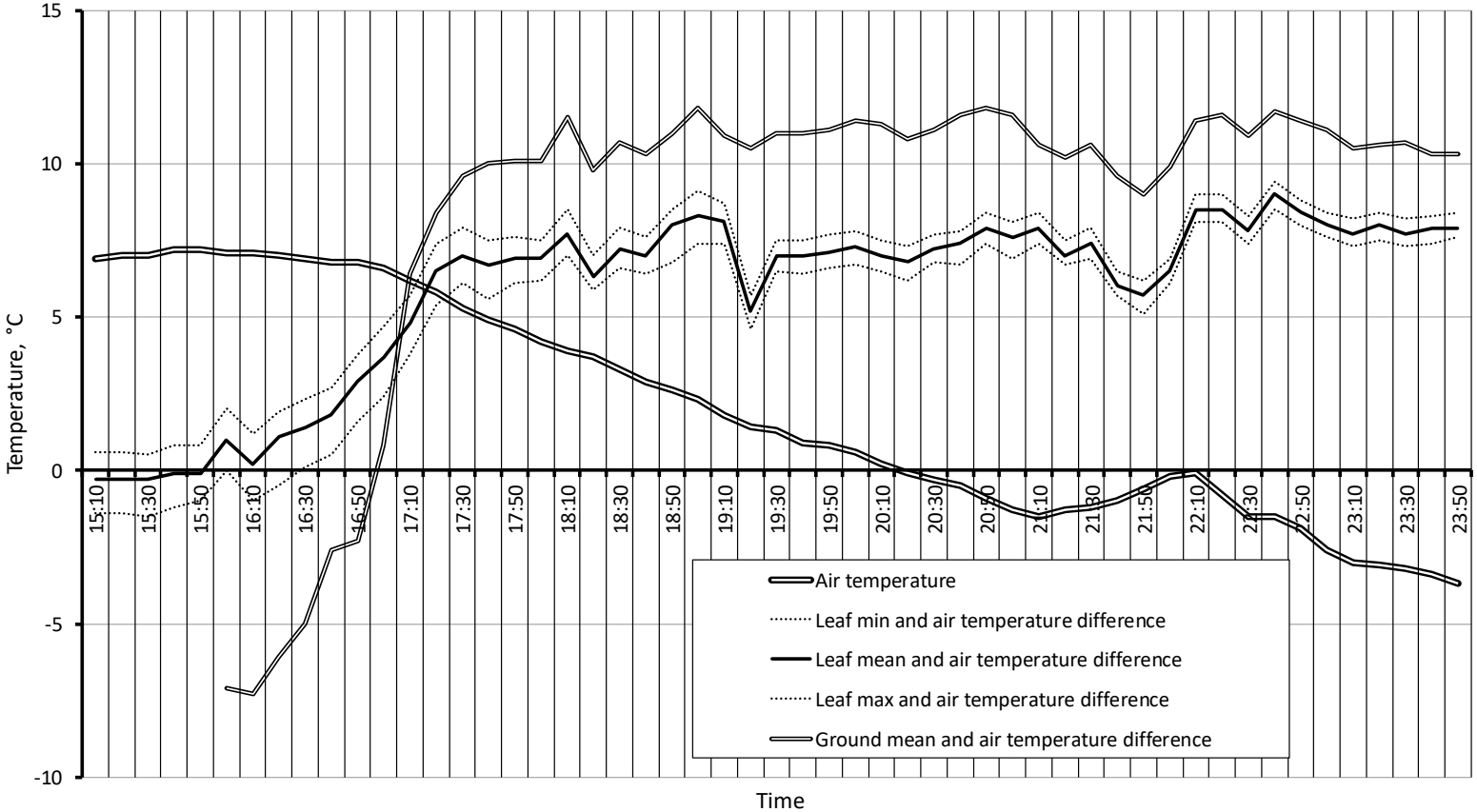

Figure 3. Temperature differences between the air, plant leaf and ground surface.

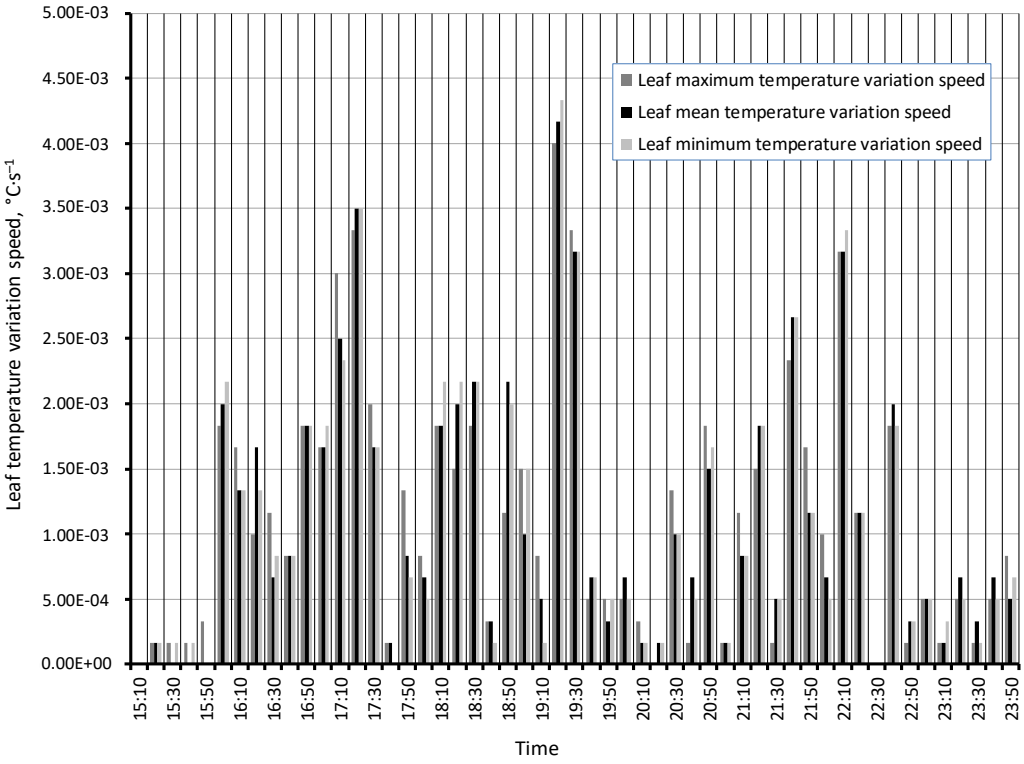

Figure 4. The speed of change of strawberry leaf temperatures.

We propose that the thermal imaging or infrared radiation measurement should be used simultaneously with air temperature measurements for more exact timing of night frost prevention measures at strawberry cultivation.

CONCLUSIONS

Our test affirms that IR thermography, as a method that is based on non-invasive, simply handled tools with specific analysing software is applicable for strawberry plant surface temperature dynamics measurements *in situ* in negative radiative balance conditions. The IR camera applied in our experiment is suitable for these purposes.

We found that in night frost climatic conditions the temperature of strawberry leaf surface is considerably (up to 9 K) lower than the air temperature. That confirms the need to apply the thermal radiation measurement equipment and to include radiative heat-balance theory for establishing plants' surface temperatures and investigation of plants' behaviour.

The thermal imaging or infrared radiation measurement should be used simultaneously with air temperature measurements for more exact timing of night frost prevention measures for plants, especially at strawberry cultivation.

The results of test show, that solely dew point and air temperatures measurements are not sufficient to produce frost alerts.

The difference of air and leaf surface temperatures is considerably higher than the possible maximum measurement error in case of thermal camera. To produce the

correctly timed frost alerts, comparatively cheap widely used commercial IR equipment is suitable.

For more deep investigation of leaves' temperature dynamics and behaviour of plants, additional night frost radiative balance research is needed.

ACKNOWLEDGEMENTS. The authors would like to thank the participating farmers for their support during farm visits. This research did not receive any specific grant from funding agencies in the public, commercial, or not-for-profit sectors.

REFERENCES

Aubrecht, D., Helliker, B., Goulden, M., Roberts, D., Still, C. & Richardson, A. 2016. Continuous, long-term, high-frequency thermal imaging of vegetation: Uncertainties and recommended best practices. *Agricultural and forest Meteorology* **228–229**, 315–326.

Barfield, B., Walton, L. & Lacey, R. 1981. Prediction of sprinkler rates for night-time radiation frost. *Agricultural and forest meteorology* **2(**4), 1–9.

Businger, J. 1964. Frost protection with irrigation. *Meteorological Monographs* **6(**28) 74–80.

Costa, M., Grant, O & Chaves, M. 2013. Thermography to explore plant – environment interactions. *Journal of Experimental Botany* **13(**64), 3937–3949.

Chiachung Chen. 2015. Determining the Leaf Emissivity of Three Crops by Infrared Thermometry. *Sensors* 1**5**, 11387–11401.

FLIR. User's manual. 2011. Publ. No. 1558550, Rev. a557. *Flir Systems, Inc*., 308 p.

Gerber, J. & Harrison, D. 1964. Sprinkler irrigation for cold protection of Citrus. *Transactions of the ASAE*, 464–468 pp.

Hamer, P. 1986. The heat balance of apple buds and blossom. Part III. The water requirements for evaporative cooling by overhead sprinkler irrigation. *Agricultural and Forest Meteorology* **37**, 175–188.

Jones, H., Archer, N., Rotenberg, E. & Casa, R. 2003. Radiation measurement for plant ecophysiology. *Journal of Experimental Botany* **384**(54), 879–889.

Jones, H. & Rotenberg, E. 2011. Energy, radiation and temperature regulation in plants. In: eLS. John Wiley & Sons Ltd.

Laury Chaerle, Dominique Van Der Straeten. 2000. Imaging Techniques and the Early Detection of Plant Stress. *Trends in Plant Science* **5(**11), 495–501.

Maes, W. & Steppe, K. 2012. Estimating evapotranspiration and drought stress with ground-based thermal remote sensing in agriculture: a review. *Journal of Experimental Botany* **13(**63), 4671–4712.

Maria, F. Buitrago, Thomas A. Groen, Christoph A. Hecker, Andrew K. Skidmore. 2016. Changes in Thermal Infrared Spectra of Plants Caused by Temperature and Water Stress. ISPRS *Journal of Photogrammetry and Remote Sensing* **111**, 22–31.

Perry, K. 1986. FROSTPRO, a model of overhead irrigation rates for frost/freeze protection of apple orchards. *HortScience* **21**(4), 1060–1061.

Perry, K. 1994. Frost/freeze protection for horticultural crops. Horticulture Information Leaflets. North Carolina A&T State University, 9.

Standard test methods for measuring and compensating for reflected temperature using infrared imaging radiometers. 1998. *An American National Standard*. ASTM, USA, 3.

Usamentiaga, R., Venegas, P., Guerediaga, J., Vega, L. & Molleda, J. 2014. Infrared thermography for temperature measurement and non-destructive testing. *Sensors* **14**(7), 12305–12348.